ACI STRUCTURAL JOURNAL TECHNICAL PAPER

Title no. 95-S14

Prediction of Failure Load of R/C Beams Strengthened with FRP Plate Due to Stress Concentration at the Plate End



by Amir M. Malek, Hamid Saadatmanesh, and Mohammad R. Ehsani

Epoxy-bonding a composite plate to the tension face is an effective technique for repair and retrofit of reinforced concrete beams. Experiments have indicated local failure of the concrete layer between the plate and longitudinal reinforcement in retrofitted beams. This mode of failure is caused by local stress concentration at the plate end as well as at the flexural cracks. This paper presents a method for calculating shear and normal stress concentration at the cutoff point of the plate. This method has been developed based on linear elastic behavior of the materials. The effect of the large flexural cracks along the beam has also been investigated. The model has been used to find the shear stress concentration at these cracks. The predicted results have been compared to both finite element method and experimental results. The analytical models provide closed form solutions for calculating stresses at the plate ends that can easily be incorporated into design equations.

Keywords: analytical modeling; epoxy; fiber composites; interfacial stress; local failure; peeling failure; plating; repair; retrofit; stress concentration.

INTRODUCTION

In recent years, repair and retrofit of existing structures have been among the most important challenges in civil engineering. The primary reasons for strengthening of structures include: upgrading of resistance to withstand underestimated loads; increasing the load-carrying capacity for higher permit loads; eliminating premature failure due to inadequate detailing; restoring lost load carrying capacity due to corrosion or other types of degradation caused by aging, etc. Different techniques have been developed to retrofit a variety of structural deficiencies. For concrete columns, lateral confinement has been provided by means of steel jackets or fiber-reinforced-plastic (FRP) wraps.[1,2] For concrete beams, flexural and shear strengthening have been performed by epoxy bonding steel or FRP plates to the tension face and the web of the beams, as shown in Fig. 1. Steel plates have been used in many countries for flexural strengthening of concrete beams for several years.[3-5] The main disadvantage of using steel plate is corrosion of steel which adversely affects the bond at the steel concrete interface. The problem is more severe for bridges where deicing chemicals are commonly used during cold seasons. In order to eliminate the corrosion problem, steel plate has been replaced by FRP plate.

Fiber reinforced plastic materials have been used successfully in the aerospace industry for several decades. These materials can be made from different types of fibers and matrices.[6] FRP plates are not prone to electrochemical corrosion as is steel. Furthermore, they can be formed, fabricated, and bonded easier than steel plates. FRPs generally behave linearly elastic to failure. The mechanical properties of FRP vary with the type and orientation of the reinforcing fibers. Therefore, the fibers can be placed in any orientation to maximize the strength in a desired direction. In this paper, only unidirectional FRP is used for developing the analytical models.

In strengthening reinforced concrete beams with FRP plates, different failure modes have been reported.[7,8] These modes can be divided into two general categories of "flexural" and "local" failures. "Flexural failure" is defined as concrete crushing in compression or plate rupturing in tension. "Local failure" is defined as the peeling of the FRP plate at the location of high interfacial stresses and shear failure of the concrete layer between the plate and the longitudinal reinforcement, as shown in Fig. 2. Flexural failure has been already investigated analytically.[9] This paper concentrates on analytical modeling of "local failure." Since in many cases the failure of retrofitted beams is governed by the "local" failure, the investigation of the stresses at the concrete/FRP interface is an important issue in the analysis and design of this type of beam.

Equations are presented here for calculating the shear and normal interfacial stresses. In order to verify this method, the results are compared to those of the finite element and experimental studies. Although the method has been developed based on uncracked beams, its validity for cracked beams has also been investigated.

ACI Structural Journal, V. 95, No.1, January-February 1998.
Received May 30, 1996, and reviewed under Institute publication policies. Pertinent discussion will be published in the May-June 1998 *ACI Structural Journal* if received by January 1, 1998.

Amir M. Malek *received his PhD from the Department of Civil Engineering and Engineering Mechanics at the University of Arizona, Tucson, and he is currently an adjunct faculty member in the same department. He was formerly a lecturer in the Civil Engineering Department at the Isfahan University of Technology, Iran. His current research area is the analytical study of reinforced concrete structures strengthened with composite plates.*

Hamid Saadatmanesh *is an Associate Professor of Civil Engineering in the Department of Civil Engineering and Engineering Mechanics at the University of Arizona, Tucson. His primary area of research is in applications of advanced composite materials for strengthening and rehabilitating structures. He is a member and past secretary of ACI Committee 440, Fiber Reinforced Plastic Reinforcement.*

Mohammad R. Ehsani *is a Professor of Civil Engineering at the Department of Civil Engineering and Engineering Mechanics at the University of Arizona, Tucson. He is a member of ACI Committee 408, Bond and Development of Reinforcement. He is also Secretary of ACI Committee 352, Joints and Connection in Monolithic Structures. Dr. Ehsani is a registered Professional Engineer in Arizona and California.*

RESEARCH SIGNIFICANCE

In flexural strengthening of reinforced concrete beams with epoxy-bonded FRP plates, local failure in the concrete layer between the steel reinforcement and the composite plate has been observed in experiments. This type of failure prevents the strengthened beam from reaching its ultimate flexural capacity, and therefore it must be included in design considerations. This failure mode is unique to plated beams and is caused by shear and normal stress concentrations at the plate end and at the flexural cracks present along the beam. Closed form solutions of stress concentrations are required in developing design guidelines for strengthening reinforced concrete beams with FRP plates.

ANALYTICAL MODELS

In this section, analytical models are developed for predicting the shear and normal stresses at the concrete/FRP interface. The following assumptions are made: linear elastic and isotropic behavior for FRP, epoxy, concrete, and steel reinforcement; complete composite action between plate and concrete (no slip); and linear strain distribution through the full depth of the section. The above assumptions do not oversimplify the behavior of this system since the plate cutoff point is usually taken near the inflection or points of zero moments where the normal stresses are generally low and justify the assumptions of linear elastic for the materials.

Shear stress

The interfacial shear stress between FRP plate and epoxy can be calculated by considering the equilibrium of an infinitesimal part of the FRP plate, as shown in Fig. 3. In this figure, $\tau(x)$ and $f_n(x)$ are shear and normal stresses, respectively. The shear stress can be defined by:

$$\tau(x) = \frac{df_p(x)}{dx} t_p \tag{1}$$

where $f_p(x)$ = tensile stress in FRP plate; and t_p = thickness of plate.

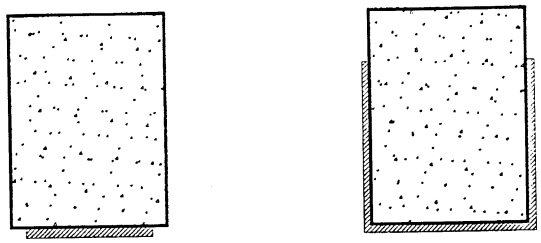

Fig. 1—Flexural and shear strengthening of reinforced concrete beams

Fig. 2—Local failure in reinforced concrete beams strengthened with FRP plates

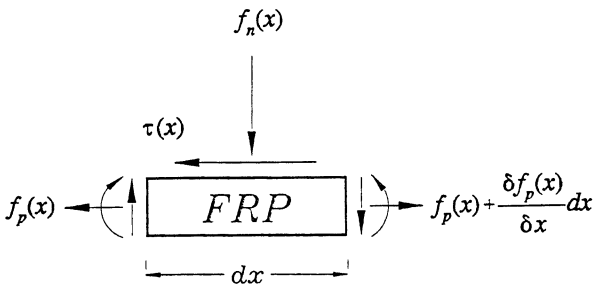

Fig. 3—Stresses acting on FRP plate

Assuming linear elastic behavior, Eq. (1) can be rewritten as:

$$\frac{df_p(x)}{dx} = \frac{G_a}{t_p}\left(\frac{du}{dy} + \frac{dv}{dx}\right) \tag{2}$$

where u and v = horizontal and vertical displacements in the adhesive layer, respectively; G_a = shear modulus of elasticity of the adhesive layer; x and y = measured along the longitudinal axis and perpendicular to the longitudinal axis of FRP plate, respectively.

Differentiating Eq. (2) with respect to x, results in:

$$\frac{d^2f_p(x)}{dx^2} = \frac{G_a}{t_p}\left(\frac{d^2u}{dxdy} + \frac{d^2v}{dx^2}\right) \tag{3}$$

The relationship between the bending moment, M, and the flexural deflection is given by:

$$\frac{d^2v}{dx^2} = \frac{M}{E_c I_{tr}} \tag{4}$$

where E_c = elastic modulus of concrete in tension; and I_{tr} = moment of inertia of transformed section based on concrete. Furthermore, $d^2u/dxdy$ can be expressed as:

$$\frac{d^2u}{dxdy} \cong \frac{1}{t_a}(\varepsilon_p - \varepsilon_c) \tag{5}$$

where ε_p and ε_c = interfacial strains in the lower and upper faces of the epoxy layer; and t_a = thickness of epoxy layer. Therefore, Eq. (2) can be written as:

$$\frac{d^2 f_p(x)}{dx^2} = \frac{G_a}{t_p}\left(\frac{\varepsilon_p}{t_a} - \frac{\varepsilon_c}{t_a} + \frac{M}{E_c I_{tr}}\right) \tag{6}$$

The magnitude of the third term in the parentheses is relatively small as compared to the other terms and therefore it can be neglected. Eq. (6) is then reduced to:

$$\frac{d^2 f_p(x)}{dx^2} = \frac{G_a}{t_a t_p}(\varepsilon_p - \varepsilon_c) \tag{7}$$

where $\varepsilon_p = f_p(x)/E_p$ and $\varepsilon_c = f_c(x)/E_c$, assuming uncracked section and using the corresponding stress-strain relationships for concrete and FRP plate; E_p = elastic modulus of plate; $f_c(x)$ = tensile stress in the bottom of the concrete beam. The governing differential equation for the tensile stress in the plate can be expressed as:

$$\frac{d^2 f_p(x)}{dx^2} - \frac{G_a f_p(x)}{t_a t_p E_p} = -\frac{f_c(x) G_a}{t_a t_p E_c} \tag{8}$$

The solution of the above equation is given by:

$$f_p(x) = C_1 \sinh(\sqrt{A}x) + C_2 \cosh(\sqrt{A}x) + b_1 x^2 + b_2 x + b_3 \tag{9}$$

where

$$A = \frac{G_a}{t_a t_p E_p}$$

and

$$b_1 = \frac{y a_1 E_p}{I_{tr} E_c}$$

$$b_2 = \frac{y E_p}{I_{tr} E_c}(2a_1 L_o + a_2)$$

$$b_3 = E_p\left[\frac{y}{I_{tr} E_c}(a_1 L_o^2 + a_2 L_o + a_3) + 2b_1 \frac{t_a t_p}{G_a}\right]$$

In developing the above solution, the origin of x has been assumed at the cutoff point of the plate. Furthermore, bending moment can be expressed by:

$$M(x_0) = a_1 x_0^2 + a_2 x_0 + a_3 \tag{10}$$

where the origin of x_0 is arbitrary, and can be assumed at any convenient point at a distance L_o from the cutoff point. In other words, $x_0 = x + L_o$; $\bar{y}$ = distance from neutral axis of the strengthened section to center of FRP plate; and C_1, C_2 = integration constants.

Substituting the expression for $f_p(x)$ given by Eq. (9) into Eq. (1), results in:

$$\tau(x) = t_p[C_1\sqrt{A}\cosh(\sqrt{A}x) + C_2\sqrt{A}\sinh(\sqrt{A}x) + 2b_1 x + b_2] \tag{11}$$

Constants of integration C_1 and C_2 are evaluated using the following boundary conditions: the first boundary condition is evaluated at $x = 0$ where the plate ends. At this point $f_p(x) = 0$. The second boundary condition is evaluated at the point where shear force in the beam is zero, i.e.:

$$\tau(L_s) = 0 \text{ or } \left.\frac{df_p(x)}{dx}\right|_{L_s} = 0$$

where L_s = distance to the point of zero shear force measured from the plate end.

Using the above boundary conditions the following expressions for C_1 and C_2 can be obtained:

$$C_1 = \frac{b_3\sqrt{A}\sinh(\sqrt{A}L_s) - 2b_1 L_s - b_2}{\sqrt{A}\cosh(\sqrt{A}L_s)} \tag{12}$$

$$C_2 = -b_3$$

A parametric study of variables in Eq. (12) revealed that generally, $\sinh(\sqrt{A}L_s)$ and $\cosh(\sqrt{A}L_s)$ are equal and have very large values compared to the other terms in the numerator. Therefore, C_1 can be simplified to:

$$C_1 = b_3$$

Using C_1 and C_2 in Eq. (11), the shear stress is expressed by:

$$\tau(x) = t_p[b_3\sqrt{A}\cosh(\sqrt{A}x) - b_3\sqrt{A}\sinh(\sqrt{A}x) + 2b_1 x + b_2] \tag{13}$$

The maximum shear stress occurs at the cutoff point ($x = 0$):

$$\tau_{max} = t_p(b_3\sqrt{A} + b_2) \tag{14}$$

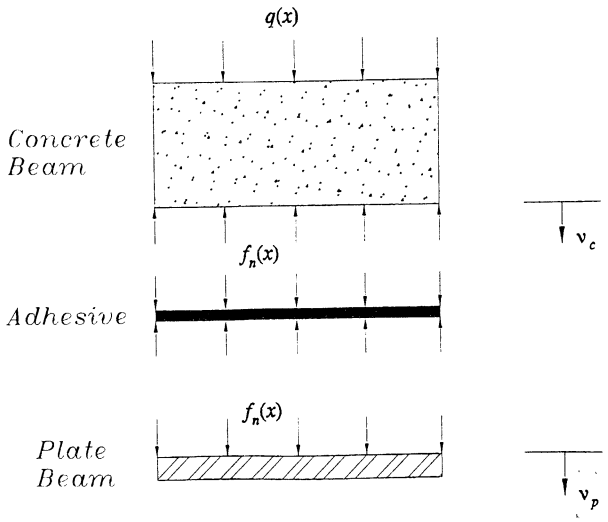

Fig. 4—Normal stresses acting on the isolated concrete and plate beams

Normal (peeling) stress

Considering concrete beam and FRP plate as two isolated beams ("concrete beam" and "plate beam") connected together by the adhesive layer as shown in Fig. 4, the fourth order differential equation for each beam can be expressed as:

$$-E_c I_c \frac{d^4 v_c}{dx^4} = q - b_p f_n(x) \tag{15}$$

$$-E_p I_p \frac{d^4 v_p}{dx^4} = b_p f_n(x) \tag{16}$$

where v_p and v_c = deflection of FRP plate and concrete beam, respectively; I_p, I_c = moment of inertia of plate and concrete beam; b_p = width of FRP plate; q = distributed load on the concrete beam; and $f_n(x)$ = normal stress in the epoxy layer. Considering deformation in the epoxy layer, $f_n(x)$ can be expressed as:

$$f_n(x) = K_n(v_p - v_c) \tag{17}$$

where $K_n = E_a/t_a$; E_a = modulus of elasticity of adhesive; and t_a = thickness of adhesive.

Differentiating Eq. (17) four times results in:

$$\frac{d^4 f_n(x)}{dx^4} = K_n\left(\frac{dv_p^4}{dx^4} - \frac{dv_c^4}{dx^4}\right) \tag{18}$$

Solving Eq. (15) and (16) for d^4v_c/dx^4 and d^4v_p/dx^4 and substituting the corresponding values in Eq. (18) gives the governing differential equation of the normal stress:

$$\frac{d^4 f_n(x)}{dx^4} + \frac{K_n}{E_p I_p} b_p f_n(x) = \frac{K_n}{E_c I_c} \cdot q \tag{19}$$

The solution of this fourth order linear differential equation is the summation of the homogeneous and particular solutions as given below:

$$f_n(x) = e^{-\beta x}[D_1 \cos(\beta x) + D_2 \sin(\beta x)] + e^{\beta x}[D_3 \cos(\beta x) + D_4 \sin(\beta x)] + \frac{qE_p I_p}{b_p E_c I_c} \tag{20}$$

where $\beta = (K_n b_p/4E_p I_p)^{0.25}$; and D_1 to D_4 = constants of integration. The term $b_p/E_c I_c$ is relatively small compared to $b_p/E_p I_p$ and has been neglected in Eq. (19). For large values of x, i.e., for the points far from the cutoff point, the normal stress and its derivatives approach zero. Since β is a positive number, the coefficient of $e^{\beta x}$ must be zero to satisfy the above condition, that is, $D_3 = D_4 = 0$. Eq. (20) is reduced to:

$$f_n(x) = e^{-\beta x}[D_1 \cos(\beta x) + D_2 \sin(\beta x)] + \frac{qE_p I_p}{b_p E_c I_c} \tag{21}$$

Constants of integration D_1 and D_2 are calculated using the appropriate force boundary conditions at the plate cutoff point. Differentiating Eq. (17) results in:

$$\frac{d^2 f_n(x)}{dx^2} = K_n\left(\frac{d^2 v_p}{dx^2} - \frac{d^2 v_c}{dx^2}\right) \tag{22}$$

Considering the isolated "concrete beam" and the "plate beam" and using the moment-curvature relationships for these beams, Eq. (22) can be rewritten as:

$$\frac{d^2 f_n(x)}{dx^2} = \frac{K_n}{E_p I_p} M_p(x) - \frac{K_n}{E_c I_c} M_c(x) \tag{23}$$

where $M_p(x)$ and $M_c(x)$ = bending moments in the "plate beam" and "concrete beam," respectively. Differentiating Eq. (22) once more, and substituting third derivatives of displacements by the corresponding shear forces results in:

$$\frac{d^3 f_n(x)}{dx^3} = \frac{K_n}{E_p I_p} V_p(x) - \frac{K_n}{E_c I_c} V_c(x) \tag{24}$$

where: $V_p(x)$ and $V_c(x)$ = shear forces in the plate and concrete beams, respectively. The effect of the interfacial shear stress must be considered in defining the bending moment and shear forces in the isolated beams. Shear stress given by Eq. (13) multiplied by the width of the plate can be assumed as a distributed load per unit length (shear flow) along the interface of each of the beams with the adhesive layer, as shown in Fig. 5(a). The static equivalents of these distributed loads at the centroid of the beams are distributed loads plus distributed moments as shown in Fig. 5(b). Therefore, the equation of bending moment in concrete and plate beams due

to this distributed load or shear flow at the interface can be written as:

$$M_c^s(x) = -b_p\bar{y}_c t_p[b_3\sinh(\sqrt{A}x) - b_3\cosh(\sqrt{A}x) + b_1x^2 + b_2x + b_3] \quad (25)$$

$$M_p^s(x) = -b_p\frac{t_p^2}{2}[b_3\sinh(\sqrt{A}x) - b_3\cosh(\sqrt{A}x) + b_1x^2 + b_2x + b_3] \quad (26)$$

where $M_p^s(x)$ and $M_c^s(x)$ = bending moments due to shear flow at the interface of concrete and plate beams, respectively. At the end of the plate where $x = 0$; both of the above moments are zero. Therefore, the bending moment in each of the beams is only due to the externally applied loads, and is expressed by:

$$\begin{aligned} M_c &= M_o \\ M_p &= 0 \end{aligned} \quad (27)$$

where M_o = bending moment in the concrete beam at the plate end due to externally applied load. In the above expressions, it is assumed that the external load is applied to the concrete beam only.

Differentiating Eq. (25) and (26), and substituting $x = 0$, results in the shear forces in the isolated beams at the plate end:

$$V_c^s = -b_p\bar{y}_c t_p(b_3\sqrt{A} + b_2) \quad (28)$$

$$V_p^s = -\frac{1}{2}b_p t_p^2(b_3\sqrt{A} + b_2) \quad (29)$$

where V_c^s and V_p^s = shear forces at the plate end, in the concrete and plate beams due to interfacial shear stresses, respectively. The total shear force in the concrete and plate beams are calculated as:

$$\begin{aligned} V_c &= V_o + V_c^s \\ V_p &= V_p^s \end{aligned} \quad (30)$$

where V_o = shear force in the concrete beam at the plate end due to externally applied loads. Here, again it is assumed that the concrete beam alone takes the full shear due to the externally applied loads. Inserting the corresponding values given by Eq. (27) and (30) into the right side of Eq. (23) and (24), D_1 and D_2 are obtained:

$$D_1 = \frac{K_n}{E_pI_p}\cdot\frac{V_p}{2\beta^3} - \frac{K_n}{E_cI_c}\cdot\frac{V_c + \beta M_o}{2\beta^3} \quad (31)$$

$$D_2 = \frac{K_n}{E_cI_c}\cdot\frac{M_o}{2\beta^3} \quad (32)$$

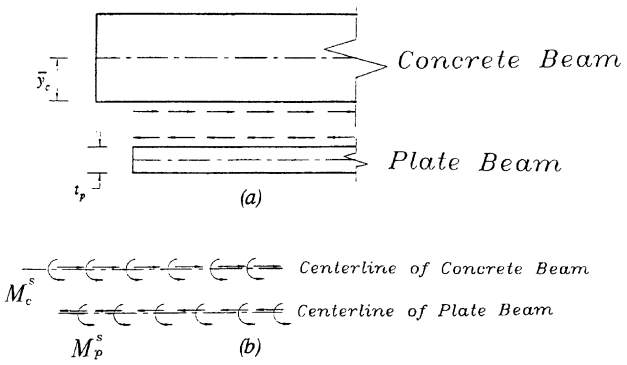

Fig. 5—(a) Shear flow acting on the isolated beams; (b) Equivalent system of distributed forces acting at the centerline of the isolated beams

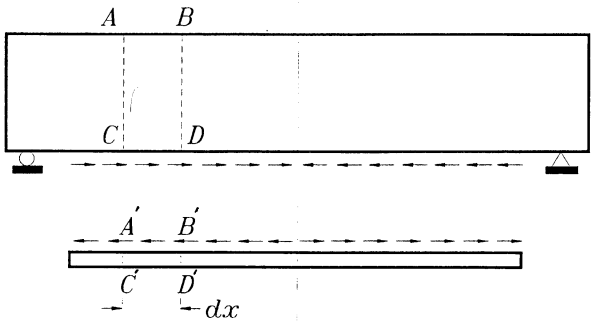

Fig. 6—Interfacial stresses acting on the isolated beams

Considering the fact that $e^{-\beta x}$ approaches zero for large values of x, the maximum normal stress occurs at the cutoff point and is expressed by:

$$f_{n_{max}} = \frac{K_n}{2\beta^3}\left(\frac{V_p}{E_pI_p} - \frac{V_c + \beta M_o}{E_cI_c}\right) + \frac{qE_pI_p}{b_pE_cI_c} \quad (33)$$

Eq. (14) and (33) express the maximum shear and normal interfacial stresses, respectively, and can provide the necessary tools for designing strengthened beam against local failure. The parameters in these equations can be simply calculated based on mechanics of materials.

Effect of shear stress concentration on flexural stresses

In order to highlight the effect of interfacial shear stresses at the concrete/plate interface on the flexural stresses in the concrete beam, the "plate beam" and the "concrete beam" are considered without externally applied loads but with self equilibriating interfacial shear stresses as shown in Fig. 6.

Isolating elements ABCD from the "concrete beam" and element A′B′C′D′ from the "plate beam," as shown in Fig. 7(a), one can see that for equilibrium of these elements, generally the existence of internal forces shown on Fig. 7(b) is necessary.

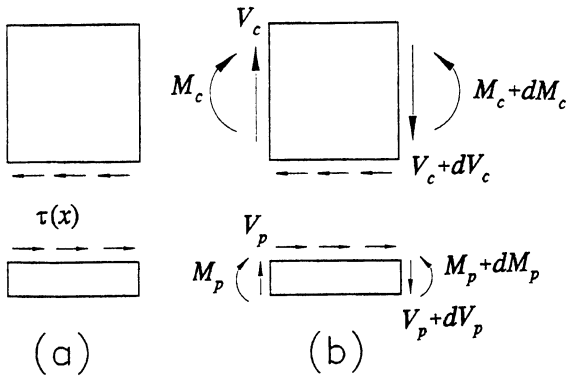

Fig. 7—(a) Isolated elements of the beams; (b) Internal forces acting on the isolated elements

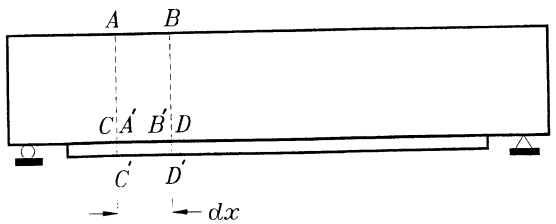

Fig. 8—Situation of isolated elements on the strengthened beam

Writing the equilibrium equation for elements in Fig. 7(b) results in:

$$\frac{dM_c}{dx} = (V_c - \tau b_p \bar{y}_c) \tag{34}$$

$$\frac{dM_p}{dx} = \left(V_p - \tau b_p \frac{t_p}{2}\right) \tag{35}$$

The strengthened beam, where the plate is attached to the concrete is shown in Fig. 8. Considering the equilibrium of this beam, the figure shows that when no external load is applied to the beam the internal forces acting on any element of the beam will be zero. In other words, the superposition of the internal forces of the concrete beam and the plate beam should add up to zero at any location along the beam, that is:

$$M_p + M_c = 0 \tag{36}$$

$$V_p + V_c = 0 \tag{37}$$

Differentiating Eq. (36) results in:

$$\frac{dM_p}{dx} + \frac{dM_c}{dx} = 0 \tag{38}$$

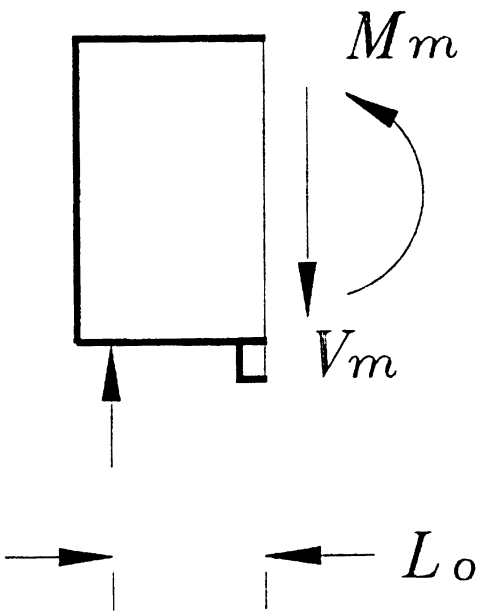

Fig. 9—Internal forces induced by the shear stress concentration at the cutoff point

Considering Eq. (34) and (35), one may write:

$$\frac{dM_p}{dx} + \frac{dM_c}{dx} - (V_p + V_c) = -\tau b_p\left(\bar{y}_c + \frac{t_p}{2}\right) \tag{39}$$

According to Eq. (37) and (38), the left-hand side of the above equation is zero, so must be the right-hand side. This can only be true if τ is zero. This is a trivial solution of the above equation, and is not of concern in this analysis. The other approach to look at this term is as an error term which must be eliminated. This elimination is performed analytically by imposing a shear force at the cutoff point in the opposite direction. However, this free body diagram will not be in equilibrium unless we have a set of forces as shown in Fig. 9. This requires a moment at the cross section expressed by:

$$M_m = L_o \tau b_p\left(\bar{y}_c + \frac{t_p}{2}\right) \tag{40}$$

In Eq. (40), the value of τ is obtained from Eq. (14), and $t_p/2$ can be neglected since its value is small compared to $\bar{y}_c$. Therefore:

$$M_m = L_o t_p b_p \bar{y}_c (b_3\sqrt{A} + b_2) \tag{41}$$

This moment is characteristic of the cutoff point in plated beam due to high shear stresses at this location. The magnitude of this moment rapidly decreases as the distance from the cutoff point increases. This moment is added to the mo-

ment from externally applied loads for the flexural design of the section at the cutoff point.

Effect of flexural cracks

Cracks play a significant role in the redistribution of the shear stresses. The same procedure to calculate shear stresses can be followed when cracks are present along the beam as shown in Fig. 10. Using Eq. (11) between two successive cracks, and assuming axial stresses in the plate at crack locations as known boundary conditions, constants C_1 and C_2 can be calculated:

$$C_1 = \frac{\bar{C}_1(b_1x_2^2 + b_2x_2 + b_3 - f_2) + \bar{C}_2(-b_1x_1^2 - b_2x_1 - b_3 + f_1)}{\bar{S}_1\bar{C}_2 - \bar{S}_2\bar{C}_1} \quad (42)$$

$$C_2 = \frac{f_2 - C_1\bar{S}_2 - b_1x_2^2 - b_2x_2 - b_3}{\bar{C}_2} \quad (43)$$

where x_1 and x_2 = coordinates of two successive cracks; f_1 and f_2 = longitudinal stress of plate at the location of the cracks; $\bar{S}_1 = \sinh(\sqrt{A}x_1)$; $\bar{S}_2 = \sinh(\sqrt{A}x_2)$; $\bar{C}_1 = \cosh(\sqrt{A}x_1)$; and $\bar{C}_2 = \cosh(\sqrt{A}x_2)$.

Defining the origin of x at the first crack, Eq. (42) is reduced to:

$$C_1 = \frac{-b_1l^2 - b_2l - b_3 + f_2 - \bar{C}_2f_1 + \bar{C}_2b_3}{\bar{S}_2} \quad (44)$$

where l = distance between cracks. Generally, $\bar{C}_2$ and $\bar{S}_2$ are equal and have large values, so the final expression for the shear stress at the crack can be simplified to:

$$\tau_{max} = t_p[b_2 + \sqrt{A}(b_3 - f_1)] \quad (45)$$

Therefore, by knowing the longitudinal stress in the FRP plate, one can find the shear stress in the adhesive layer at the same location. Considering the fact that due to opening of the cracks usually there is debonding in the adhesive layer at the crack, Eq. (45) is an important equation from the design point of view. In this equation, f_1 is predominant compared to the other terms. In other words, any approximation used in defining the tensile stress at the bottom of the concrete beam such as linear elastic behavior, has negligible effect and can be ignored.

VERIFICATION OF THE METHOD

The method is verified by comparing it to both finite element analysis and experimental results. Several researchers have reported local failure in concrete beams strengthened with FRP plates.[7,8] In this study, the beams tested by Saadatmanesh and Ehsani[8] were analyzed by using both the method described in this paper and the finite element method. For brevity, only the results of one of these beams which has failed due to local failure of concrete at the cutoff point is discussed here. The general view and also the cross section of this beam are shown in Fig. 11.

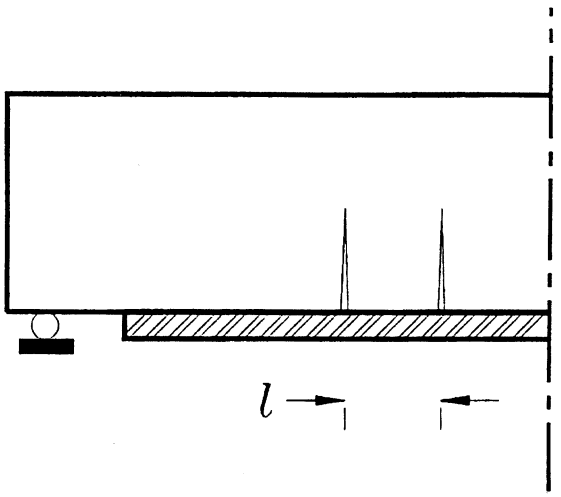

Fig. 10—Location of the cracks in the concrete beam

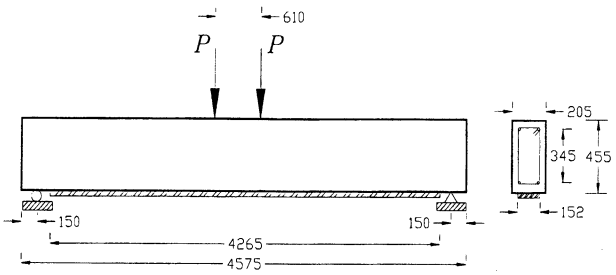

Fig. 11—General view and cross section of the test beam (Note: 1 mm = 0.0394 in.)

Table 1—Mechanical properties of materials used in the test beam

Material	Modulus of elasticity, MPa	Poisson's ratio
Concrete	27,990	0.18
Steel	200,000	0.3
FRP	37,230	0.35
Adhesive	814	0.37

Note: 1 MPa = 0.145 ksi

The mechanical properties of the materials used in the construction of the test beam are listed in Table 1.

In order to compare the results of the present method with the finite element and experimental results, it is first necessary to calculate the shear and normal stresses at the cutoff point for the test beam using the present method.

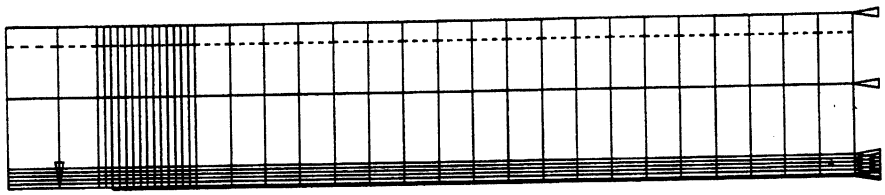

Fig. 12—General mesh definition of the test beam

Equation (13) was used to predict the interfacial shear stress. Based on an elastic analysis, which is reasonable for the end regions of the beam, the cross-sectional properties were calculated as:

$$\bar{y} = 232 \text{ mm } (9.13 \text{ in.}), I_{tr} = 1.77 \times 10^9 \text{ mm}^4 \ (4252 \text{ in.}^4)$$

The expression for the bending moment at the ultimate load of 100 kN (22.48 kips) is given by:

$$M(x_o) = 100{,}000\, x_o$$

where the origin of x_o is defined at the left support. Therefore, the coefficients of the polynomial given in Eq. (10) are:

$$a_1 = 0,\ a_2 = 100{,}000, \text{ and } a_3 = 0$$

Using Eq. (9) the following parameters are calculated:

$$b_1 = 0,\ b_2 = 0.0174, \text{ and } b_3 = 2.70$$

Subsequently, C_1 and C_2 are obtained as:

$$C_1 = 2.70, \text{ and } C_2 = -2.70$$

Knowing $G_a = 297$ MPa (43 ksi), $t_a = 1.5$ mm (0.06 in.), and $t_p = 6$ mm (0.236 in.), the constant A is calculated:

$$A = 8.96 \times 10^{-4}$$

The equation of shear stress distribution along the interface can now be expressed by:

$$\tau(x) = 0.4825 \cosh (0.0298 \text{ x}) - 0.4825 \sinh (0.0298x) + 0.1045$$

and the tensile stress in the FRP plate can be written as:

$$f_p(x) = 2.7 \sinh (0.0298x) - 2.7 \cosh (0.0298x) + 0.0174x + 2.7$$

The maximum shear stress at the cutoff point is calculated by evaluating shear stress at $x = 0$: $\tau_{max} = 0.587$ MPa (0.085 ksi).

The cross-sectional properties of "concrete beam" and "plate beam" are as follows:

$$\bar{y}_c = 227.5 \text{ mm } (8.96 \text{ in.}), I_c = 1.61 \times 10^9 \text{ mm}^4 \ (3868 \text{ in.}^4)$$

$$\bar{y}_p = 3 \text{ mm } (0.118 \text{ in.}), I_p = 2736 \text{ mm}^4 \ (0.00657 \text{ in.}^4)$$

The following can also be obtained:

$$K_n = 542.3 \text{ MPa/mm } (1997 \text{ ksi/in.}),$$
$$\beta = 0.1192 \text{ mm}^{-1} \ (3.028 \text{ in.}^{-1}).$$

Therefore, using Eq. (30), (31), and (32) one can obtain the following values:

$$V_c = 79.667 \text{ kN } (17.91 \text{ kips}); V_p = -0.268 \text{ kN } (0.062 \text{ kips});$$

$$D_1 = -0.427 \text{ MPa } (0.062 \text{ ksi}); D_2 = 0.00656 \text{ MPa } (0.000951 \text{ ksi}).$$

The equation for the normal stress is obtained as:

$$f_n(x) = e^{-0.1192x} [-0.427\cos(0.1192x) + 0.00656 \sin(0.1192x)]$$

At the cutoff point ($x = 0$) the maximum value of normal stress is obtained as:

$$f_{n,max} = -0.427 \text{ MPa } (0.062 \text{ ksi})$$

The negative sign shows tensile stress.

Comparison with finite element analysis

The "ABAQUS" Finite Element program was also used to analyze the test beam (ABAQUS, Version 5.4, 1994).

Due to the symmetry of the beam, only half of the beam was analyzed with appropriate constraints at the centerline, as shown in Fig. 12. Rebars were modeled as one-dimensional bar elements. Different meshes were used for the analysis and the results of three typical cases are discussed here.

Case I: 4-node elements with one layer of elements in the adhesive.

Case II: 8-node serendipity elements with one layer of elements in the adhesive.

Case III: 8-node serendipity elements with five layers of elements in the adhesive.

The mesh definition around the cutoff point for Case III is shown in Fig. 13.

The results of the finite element analysis together with the closed form solution (present method) for interfacial shear and normal stresses as well as the longitudinal stresses of the plate, are shown in Fig. 14(a), (b), and (c), respectively. It can be concluded that only a very fine mesh can show the descending branch in the shear stress very close to the cutoff

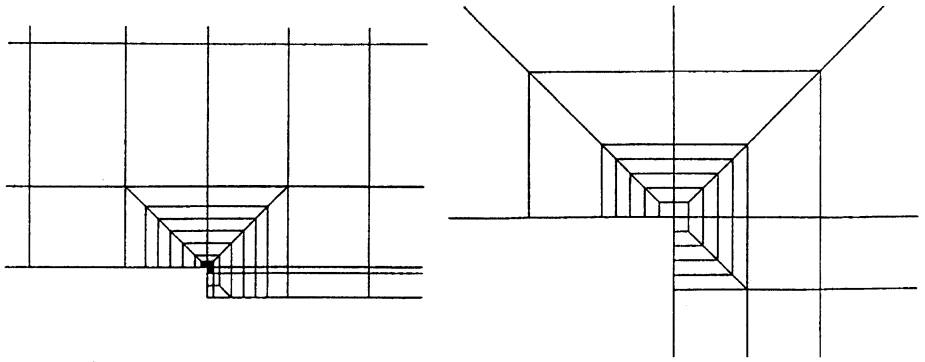

Fig. 13—Mesh definition around the cutoff point (Case III)

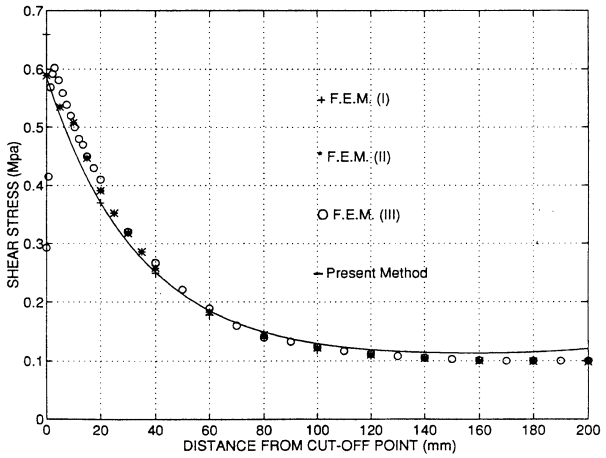

(a) Interfacial shear stress

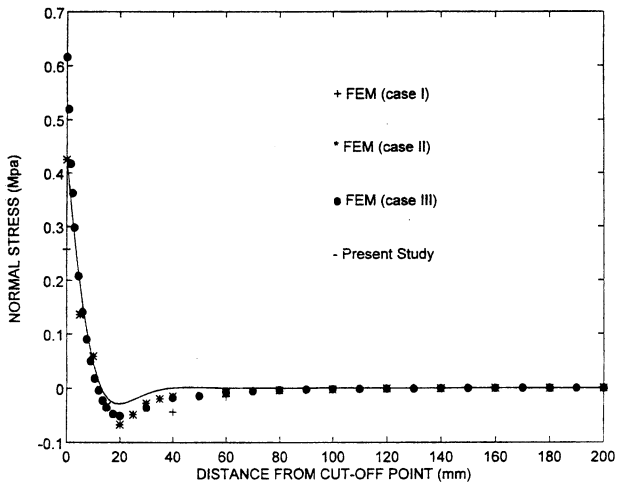

(b) Interfacial normal stress

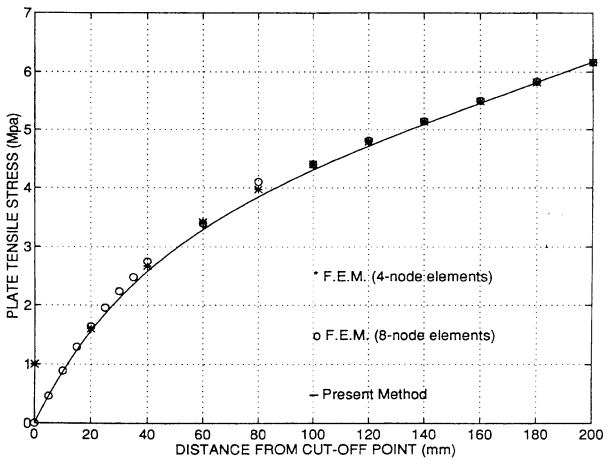

(c) tensile stress of the plate

Fig. 14—Comparison of the present method to FEM: (a) interfacial shear stress, (b) interfacial normal stress, and (c) tensile stress of the plate (Note: 1 MPa = 0.145 ksi; 1 mm = 0.0394 in.)

point. However, the maximum shear stress predicted by this method is in good agreement to the results of the finite element analysis. It is also concluded that shear stress concentration at the cutoff point rapidly vanishes when moving toward the center of the beam.

The results of the normal stress show slightly more deviation from the finite element results at the cutoff point. However, at the location of maximum stresses, which is used for design, the agreement between the finite element results and the present method is good as can be seen from Fig. 15.

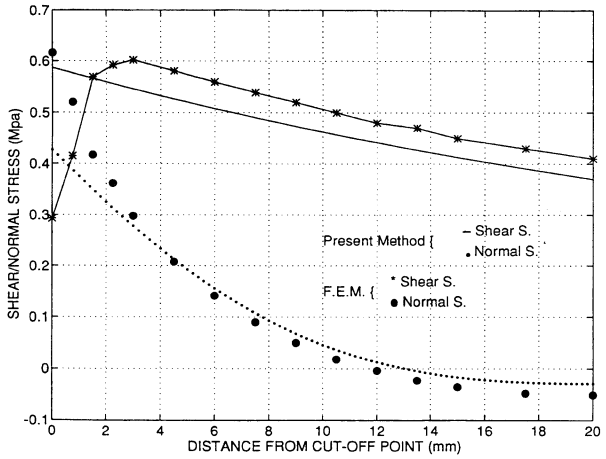

Fig. 15—Comparison of the stresses around the cutoff point in a larger scale (1 MPa = 0.145 ksi; 1 mm = 0.0394 in.)

Table 2—Variation of stresses due to orthotropic behavior of the plate

Normalized shear modulus (G_o / G_I)	Normalized shear stress (τ_o / τ_I)	Normalized normal stress (f_o / f_I)
0.1	0.942	1.07
0.2	0.967	1.10
0.4	0.984	1.08
0.6	0.993	1.05
0.8	0.998	1.03
1	1	1

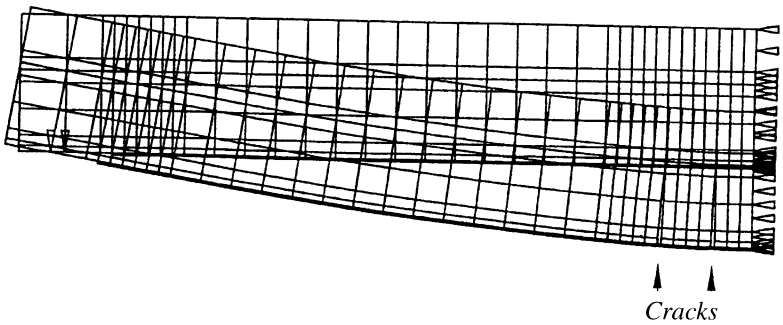

Fig. 16—Mesh definition and the location of the cracks

Effect of flexural cracks—Cracking is one of the major characteristics of concrete that affects analysis and design procedures. In order to investigate the effect of large flexural cracks on the distribution of stresses in a beam strengthened with FRP plates, the beam was analyzed assuming that two cracks were present. Mesh definition and location of the predefined flexural cracks are shown in Fig. 16.

Eight-node elements were used, and intermediate nodes of the elements around the crack tip were defined at quarter points to simulate the stress singularity at this point.[10] The average plate tensile stress at cracks 1 and 2 was 700 MPa (101.52 ksi) and 726 MPa (105.29 ksi) based on the finite element analysis. Using Eq. (44), the calculated shear stresses are 112.50 (16.32 ksi) and 116.84 MPa (16.95 ksi), respectively. The maximum shear stress in the adhesive layer around these cracks obtained by the finite element analysis was 105 MPa (15.23 ksi) and 112 MPa (16.24 ksi), which shows a good agreement. Finite element results also showed that there is compressive normal stress accompanied by shear stress, but normal stress does not show high concentration like that at the cutoff point. According to this analysis the increase in the shear stress at the cutoff point due to cracks was negligible.

Parametric study for isotropic and orthotropic behaviors of FRP plate—A parametric study was carried out to investigate the effect of unisotropy of the plate on the shear and normal stress concentrations. The test beam had unidirectional FRP plate which results in orthotropic behavior of the plate. This study showed that the variation of elastic modulus in transverse direction does not have a significant effect on shear and normal stresses. The variation of the shear modulus of elasticity, however, can somewhat change these stresses as shown in Table 2. Assuming isotropic behavior for the plate (based on longitudinal direction) results in an upper bond on the magnitude of shear stress which is a conservative solution. The variation of normalized shear and normal stress (with respect to isotropic behavior) against normalized shear modulus (with respect to isotropic case) are shown in Table 2. Where in this table subscripts *I* and *o* refer to isotropic and orthotropic.

Comparison with experimental results

According to the method presented in this paper, the shear and normal stresses at the cutoff point of the test beam are calculated as 0.586 MPa (0.085 ksi) and 0.427 MPa (0.062 ksi), respectively. The flexural stress in the concrete at the end of the plate, considering the increase in moment, M_m, is calculated as 2.545 MPa (0.369 ksi). Using these values, the principal stresses are obtained as 2.696 MPa (0.391 ksi) and 0.276 MPa (0.040 ksi), respectively. A biaxial failure model for concrete[11,12] shows a tensile strength of 3.11 MPa (0.451 ksi) for the concrete used in making the test beam (f'_c = 34.32 MPa). Comparing these results (2.696 MPa vs. 3.11 MPa) shows 13 percent difference

which is due to the approximations made in the model as well as the linear elastic behavior assumed in the method presented in this paper.

CONCLUSIONS

Shear and normal stress concentrations near the cutoff point of the FRP plate and also flexural cracks must be considered in the design of reinforced concrete beams strengthened with epoxy bonded FRP plates. These stresses may lead to failure modes such as peeling and debonding of the plate or local failure in the concrete layer between the FRP plate and longitudinal reinforcements of the beam. The method presented in this paper can be used to predict the distribution of shear and normal stress at the interface of the plate and the adhesive throughout the entire length of the plate and particularly the location of the cutoff point. The maximum values of these stresses which are important from the design point of view are given by the following simple equations:

$$\tau_{max} = t_p(b_3\sqrt{A} + b_2)$$

$$f_{n,max} = \frac{K_n}{2\beta^3}\left(\frac{V_p}{E_pI_p} - \frac{V_c + \beta M_o}{E_cI_c}\right) + \frac{qE_pI_p}{b_pE_cI_c}$$

The method has been developed based on linear elastic behavior of the concrete. However, the effect of flexural cracks has been investigated and included in this study. The effect of anisotropic behavior of FRP plate on stress distribution has been studied as well. It was concluded that the isotropic assumption for the behavior of FRP plate, used in developing this method, is acceptable. The method was applied to a beam that had been tested and had failed due to local failure of the concrete layer between the FRP plate and longitudinal reinforcement. The results of the method presented in this paper indicate a good agreement with both finite element and experimental results.

NOTATION

A = parameter used in shear/normal stress equations
$a_{1\text{-}3}$ = coefficient of bending moment polynomial
b_p = width of FRP plate
$b_{1\text{-}3}$ = parameters used in shear/normal stress equations
$C_{1\text{-}2}$ = integration constants
$\bar{C}_{1\text{-}2}$ = coefficient related to crack location
$D_{1\text{-}4}$ = integration constants
E_a = elastic modulus of epoxy (adhesive)
E_c = elastic modulus of concrete
E_p = elastic modulus of FRP plate
f_c = tensile stress in the concrete beam
f_n = normal stress in the epoxy layer
f_p = tensile stress in the FRP plate
f'_c = compressive strength of concrete
$f_{1\text{-}2}$ = tensile stress in the FRP plate at the location of the cracks
G_a = shear modulus of epoxy
I_c = moment of inertia of concrete beam
I_p = moment of inertia of plate beam
I_{tr} = moment of inertia of transformed section
K_n = normal stiffness per unit area of epoxy
L_o = distance between origin of xo and cutoff point
L_s = distance between the point of zero shear force and the cutoff point
l = distance between two successive cracks
M = bending moment
M_c = bending moment in the concrete beam
M_p = bending moment in the plate beam
M_o = bending moment in the concrete beam at the cutoff point due to external load
M_c^s = bending moment in the concrete beam due to shear flow
M_p^s = bending moment in the plate beam due to shear flow
q = external distributed load applied on concrete beam
$\bar{S}_{1\text{-}2}$ = coefficients related to crack location
t_a = thickness of epoxy layer
t_p = thickness of the FRP plate
u = horizontal displacement in the epoxy layer
V_c = shear force in the concrete beam
V_p = shear force in the plate beam
V_o = hear force in the concrete beam at the cutoff point due to external load
V_c^s = shear force in the concrete beam due to shear flow
V_p^s = shear force in the plate beam due to shear flow
v = vertical displacement in epoxy (adhesive) layer
v_c = deflection of the concrete beam
v_p = deflection of the plate beam
x = longitudinal distance
x_o = longitudinal distance in the definition of bending moment
$\bar{y}$ = distance of the center of FRP plate to the centroid of the strengthened beam
$\bar{y}_c$ = distance between the centroid and the bottom of concrete beam
β = coefficient used in normal stress definition
ε_c = axial strain at the interface of concrete and epoxy
ε_p = axial strain at the interface of FRP plate and epoxy

ACKNOWLEDGEMENTS

The work presented in this paper was partially supported by the National Science Foundation (NSF) under Grant No. MSS-925734-4. The support of the National Science Foundation is greatly appreciated. The opinions, findings, and conclusions outlined in this paper are those of the authors and do not represent the views of NSF.

REFERENCES

1. Priestly, M. J.; Fyfe, E.; and Seible, F., "Column Retrofit Using Fiberglass/Epoxy Jackets," *First Annual Seismic Research Workshop*, CALTRANS, Sacramento, 1991, pp. 217-224.

2. Saadatmanesh, H.; Ehsani, M. R.; Li, M. W., "Strength and Ductility of Concrete Columns Externally Reinforced with Fiber Composite Straps," *ACI Structural Journal*, Vol. 91, No. 4, July-Aug. 1994, pp. 434-447.

3. Dussek, T. J., "Strengthening of Bridge Beams and Similar Structures by Means of Epoxy-Resin-Bonded External Reinforcement," *Transport. Res. Rec.* 785, Transportation Research Board, 1980, pp. 21-24.

4. MacDonald, M. D., and Calder, A. J. J., "Bonded Steel Plating for Strengthening Concrete Structures," *Int. J. Adhesion and Adhesives*, Vol. 2, No. 2, 1982, pp. 119-127.

5. Swamy, R. N.; Jones, R.; Bloxham, J. W., "Structural Behavior of Reinforced Concrete Beams Strengthened by Epoxy-Bonded Steel Plates," *The Structural Engineer*, Vol. 65A, No. 2, Feb. 1987, pp. 59-68.

6. Malek, A. M., and Saadatmanesh, H., "Physical and Mechanical Properties of Typical Fibers and Resins," *Proceedings of the First International Conference on Composites in Infrastructure*, January 15-17, 1996, Tucson, AZ, pp. 68-79.

7. Ritchie, P. A.; Thomas, D. A.; Lu, Le-Wu; and Connelly, G. M., "External Reinforcement of Concrete Beams Using Fiber Reinforced Plastics," *ACI Structural Journal*, Vol. 88, No. 4, 1991, pp. 490-500.

8. Saadatmanesh, H., and Ehsani, M. R., "RC Beams Strengthened with FRP Plates I: Experimental Study," *ASCE Journal of Structural Engineering*, Vol. 117, No. 11, 1991, pp. 3417-3433.

9. An, Wei; Saadatmanesh, H.; and Ehsani, M. R., "RC Beams Strengthened with FRP Plates II: Analysis and Parametric Study," *ASCE Journal of Structural Engineering*, Vol. 117, No. 11, 1991, pp. 3434-3455.

10. Cook, R. D., *Concepts and Applications of Finite Element Analysis*, John Wiley and Sons, Inc., 1981.

11. Kupfer, H. B., and Grestle, K. H., "Behavior of Concrete Under Biaxial Stresses," *ASCE Journal of the Engineering Mechanics Division*, Vol. 99, No. EM4, 1973, pp. 853-866.

12. Nilson, A. H., and Winter, G., *Design of Concrete Structures*, 11th ed., McGraw-Hill, Inc., 1991.